EPJ Web of Conferences **69**, 00002 (2014)
DOI: 10.1051/epjconf/20146900002

Role of the Hoyle state in the ^{12}C+^{12}C fusion at low energies

P. Descouvemont[1,2,a] and M. Assunção[3,b]

[1] *Physique Nucléaire Théorique et Physique Mathématique, C.P. 229, Université Libre de Bruxelles (ULB), B 1050 Brussels, Belgium*
[2] *Instituto de Estudos Avançados da Universidade de São Paulo, Caixa Postal 72012, 05508-970, São Paulo, Brazil*
[3] *Departamento de Ciências Exatas e da Terra, Universidade Federal de São Paulo, 09972-270, Campus Diadema, São Paulo, Brazil*

Abstract. The ^{12}C+^{12}C fusion reaction is investigated in a multichannel folding model, using the density-dependent DDM3Y nucleon-nucleon interaction. The ^{12}C($0^+_1, 2^+, 0^+_2, 3^-$) states are included, and their densities are taken from a microscopic cluster calculation. Absorption to fusion channels is simulated by a short-range imaginary potential and the model does not contain any fitting parameter. We compute elastic and fusion cross sections simultaneously. The role of ^{12}C+^{12}C inelastic channels and, in particular, of the ^{12}C(0^+_1)+^{12}C(0^+_2) channel involving the Hoyle state is important even at low energies.

1 Introduction

After helium burning, a large concentration of ^{12}C in the core of massive stars leads to a rapid carbon burning phase [1]. In this phase the ^{12}C+^{12}C fusion reaction (which essentially produces α particles and protons) plays an essential role (see recent reviews in Refs. [2, 3]). A recent work, aimed at exploring the impact of current uncertainties on the ^{12}C+^{12}C reaction rate, suggests that essentially p-process abundances are affected [3].

A general problem in nuclear astrophysics is that the relevant stellar energies (referred to as the "Gamow window") are much lower than the Coulomb barrier [4–6]. Due to barrier-penetration effects, the cross sections in the Gamow region cannot be measured in the laboratory, and higher-energy data must be extrapolated down to low energies. For the ^{12}C+^{12}C reaction, the typical energies are around 2 MeV, whereas the Coulomb barrier is around 6.5 MeV. The expected cross section at 2 MeV is of the order of 10^{-11} barns. In the ^{12}C+^{12}C reaction, the situation is made more complicated owing to the presence of broad structures in the experimental cross section, even below the Coulomb barrier [7]. Extrapolations at low energies are therefore very uncertain. Recently a possible new resonance at 2.14 MeV has been reported [8], but this measurement is questioned (see Ref. [9]). Several attempts have been performed to explain the origin of these resonances [9–11].

[a] e-mail: pdesc@ulb.ac.be
[b] e-mail: massuncao@unifesp.br

Several calculations have been performed to investigate the ^{12}C+^{12}C fusion process. These calculations are based on the barrier-penetration model [12, 13] or on the ingoing-wave-boundary conditions [14]. A microscopic cluster model has been developed for fusion reactions [15]. Most fusion calculations to date are performed in a single-channel model, i.e. involving the ^{12}C ground-state only. Absorption is simulated by a phenomenological imaginary potential [16]. In light systems, however, it is known that inelastic channels may be important and require to be explicitly included in the calculation. In Ref. [17], the authors suggest that mutual excitations play an important role even at low energies, where excited channels are closed. At first sight, this effect may seem surprising since only a single channel is open. It is explained by distortion effects in the wave functions: the cross section is mostly sensitive to the inner part of the wave functions, where closed channels may have a significant amplitude.

Our goal here is to investigate the ^{12}C+^{12}C fusion in a multichannel folding method [18]. We include the ^{12}C($0^+_1, 2^+, 0^+_2, 3^-$) states, and the corresponding mutual excitations. A folding method relies on two main inputs: the nucleon-nucleon (NN) interaction and ^{12}C densities. For the NN interaction we use the density-dependent M3Y (DDM3Y) interaction [19]. Including the density dependence was shown to reduce the depth of the nucleus-nucleus potential at short distances (in Ref. [17], the authors use the original M3Y interaction and the density effect is simulated by a repulsive core). For the ^{12}C densities, we use the RGM values of Kamimura [20]. These densities (elastic and inelastic) are obtained from a microscopic triple-alpha model, and are known to provide a precise description of many scattering data. In particular the 0^+_2 state of ^{12}C has attracted much attention in recent years, since it might be considered as an α-condensate state [21]. This state is well described by the three-α microscopic calculation of Kamimura, and is expected to play a significant role in the ^{12}C+^{12}C system [22].

Our calculation is free of parameters, except for a weak dependence on the absorption potential. It provides a simultaneous description of elastic scattering and of fusion. Elastic cross sections around the Coulomb barrier are well known experimentally [23] and will serve as a test of the model, in order to assess the accuracy of the less known fusion cross section. The main results are presented in Ref.[24], and we refer to that reference for detail.

2 Theoretical background

2.1 Hamitonian and wave functions

The Hamiltonian of the system is given by

$$H = T_r + H_1(\boldsymbol{r}_i) + H_2(\boldsymbol{r}_j) + \sum_{i=1}^{A_1}\sum_{j=1}^{A_2} v_{NN}(\boldsymbol{r} - \boldsymbol{r}_i + \boldsymbol{r}_j) \tag{1}$$

where T_r is the relative kinetic energy and H_1, H_2 are the internal Hamiltonians of the colliding nuclei. In this equation, $\boldsymbol{r}$ is the relative distance between the c.m. of the nuclei, $\boldsymbol{r}_i$ and $\boldsymbol{r}_j$ are sets of coordinates associated with H_1 and H_2, and v_{NN} a nucleon-nucleon interaction.

For a given angular momentum J and parity π, a multichannel ^{12}C+^{12}C wave function is written as

$$\Psi^{JM\pi} = \frac{1}{r}\sum_{\alpha_1\alpha_2\ell I} \varphi^{JM\pi}_{\alpha_1\alpha_2\ell I}(\Omega_r) g^{J\pi}_{\alpha_1\alpha_2\ell I}(r), \tag{2}$$

where the channel wave functions are defined by

$$\varphi^{JM\pi}_{\alpha_1\alpha_2\ell I}(\Omega_r) = \left[\left[\Phi^{I_1\pi_1}_{\alpha_1} \otimes \Phi^{I_2\pi_2}_{\alpha_2}\right]^I \otimes Y_\ell(\Omega_r)\right]^{JM}. \tag{3}$$

In this expression, $\Phi_{\alpha_k}^{I_k\pi_k}$ are spinors associated with the different ^{12}C states (labels α_k refer to different excitation levels), I is the channel spin, ℓ is the relative orbital momentum, and the total parity is given by $\pi = \pi_1\pi_2(-1)^\ell$. For symmetric channels ($\alpha_1 = \alpha_2$), we have the selection rule $(-1)^{\ell+I} = 1$. In what follows, we use the index $c = (\alpha_1\alpha_2\ell I)$. and

The radial wave functions $g_c^{J\pi}(r)$ are obtained from the coupled-channel system

$$-\frac{\hbar^2}{2\mu}\Big[\frac{d^2}{dr^2} - \frac{\ell(\ell+1)}{r^2}\Big]g_c^{J\pi}(r) + \sum_{c'} V_{cc'}^{J\pi}(r)g_{c'}^{J\pi}(r) = (E - E_1^c - E_2^c)g_c^{J\pi}(r), \tag{4}$$

where μ is the reduced mass of the system, and E_i^c are the ^{12}C energies. The coupling potentials are defined as

$$V_{cc'}^{J\pi}(r) = \langle\varphi_c^{J\pi}(\Omega_r)|\sum_{i=1}^{A_1}\sum_{j=1}^{A_2} v_{NN}(\boldsymbol{r} - \boldsymbol{r}_i + \boldsymbol{r}_j)|\varphi_{c'}^{J\pi}(\Omega_r)\rangle, \tag{5}$$

where the integration is performed over Ω_r (see Ref. [25] for detail).

The coupled-channel system (4) is solved with the R-matrix method [26], which is based on an internal region, where the nuclear interaction is important, and on an external region, where it is negligible. In the internal region ($r \le a$), the radial functions $g_c^{J\pi}(r)$ are expanded over a Lagrange basis [27]. In the external region, it is given by a linear combination of Coulomb functions. The matching provides the collision matrix $\boldsymbol{U}^{J\pi}$. Notice that, at low energies, most of ^{12}C+^{12}C excited channels are closed (the first open channel is ^{12}C(0_1^+)+^{12}C(2^+) which opens at 4.44 MeV). This means that the corresponding components $g_c^{J\pi}(r)$ tend to zero at large distances. However, couplings with excited channels introduce distortion effects in the wave function, and modify the scattering matrix.

2.2 Multichannel folding potentials

The density dependence of the nucleon-nucleon nuclear interaction v_{NN} is known to account for the overlapping of the colliding nuclei. By reducing the depth of the nucleus-nucleus folding interaction, it simulates the Pauli principle and significantly improves the accuracy of the original M3Y interaction. In a coupled-channel formalism, the ^{12}C+^{12}C potentials are defined from

$$V_{\alpha_1\alpha_2,\alpha_1'\alpha_2'}(\boldsymbol{r}) = \iint d\boldsymbol{r}_1 d\boldsymbol{r}_2\, v_{NN}(\boldsymbol{s},\rho,E)\,\rho_1^{\alpha_1\alpha_1'}(\boldsymbol{r}_1)\,\rho_2^{\alpha_2\alpha_2'}(\boldsymbol{r}_2), \tag{6}$$

where $\boldsymbol{s} = \boldsymbol{r} - \boldsymbol{r}_1 + \boldsymbol{r}_2$, $\rho_k^{\alpha\alpha'}(\boldsymbol{r}_k)$ are the ^{12}C nuclear densities, and the labels α_k refer to different ^{12}C states. Equation (6) is written in a general form, where the nucleon-nucleon interaction depends on the density of the system ρ and on the energy E. The DDM3Y interaction uses the frozen density approximation, where $\rho = \rho_1(\boldsymbol{r}_1) + \rho_2(\boldsymbol{r}_2)$. The same folding formalism is applied to the Coulomb interaction. In the present work, we include the ^{12}C($0_1^+, 2^+, 0_2^+, 3^-$) states, which means that ten ^{12}C+^{12}C channels are introduced in the coupled-channel system. The densities $\rho_k^{\alpha\alpha'}(\boldsymbol{r})$ are taken from the 3α microscopic calculation of Kamimura [20]. These densities, elastic ($\alpha = \alpha'$) as well as inelastic ($\alpha \neq \alpha'$), are known to reproduce many experimental data. Details on the calculation of the folding potential can be found in the appendix.

We illustrate in Fig.1 the folding potentials for two channels, ^{12}C(0_1^+)+^{12}C(0_1^+), and ^{12}C(0_2^+)+^{12}C(0_2^+). The calculations are performed with the density-dependent DDM3Y interaction, as well as with its M3Y approximation. As expected, the DDM3Y potential reduces the short-range part due to the Pauli principle. The potentials corresponding to the ^{12}C(0_2^+)+^{12}C(0_2^+) channels extend to larger distances according to the larger radius of the Hoyle state. At the scale of the figure, the Coulomb potentials are identical for both channels.

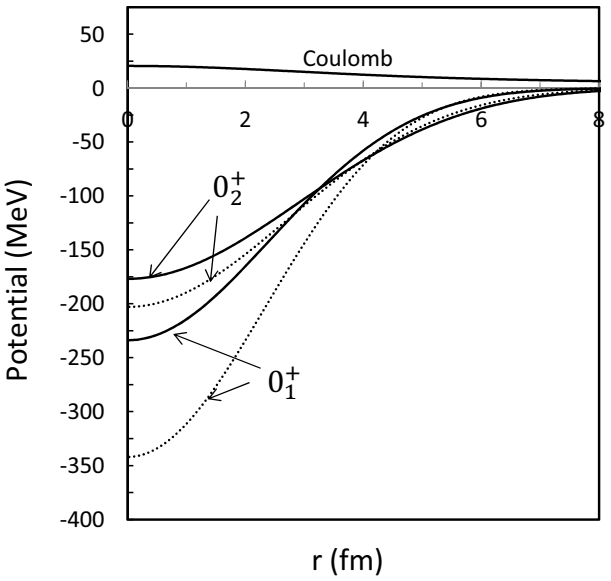

Figure 1. Folding potentials for the $^{12}C(0_1^+)+^{12}C(0_1^+)$ and $^{12}C(0_2^+)+^{12}C(0_2^+)$ channels. Solid lines correspond to the DDM3Y potential and dotted lines to the M3Y interaction.

2.3 Fusion cross sections

It is well known that an imaginary component must be added to the potential $V_{cc'}^{J\pi}$ to simulate other absorption channels. In other words, the folding (real) potential (5) is complemented in Eq. (4) as

$$V_{cc'}^{J\pi}(r) \longrightarrow V_{cc'}^{J\pi}(r) + iW_{cc'}^{J\pi}(r). \tag{7}$$

In general, the imaginary term $W_{cc'}^{J\pi}(r)$ is written as

$$W_{cc'}^{J\pi}(r) = N_I\, V_{cc'}^{J\pi}(r), \tag{8}$$

where N_I is a constant amplitude fitted to the data. However, the imaginary potential can be separated in two components: one describing inelastic channels, possibly missing in the calculation, and another associated with fusion, or compound-nucleus formation [28, 29]. In the present calculation, the coupled-channel system (4) explicitly includes inelastic channels in a wide energy range. Accordingly, these channels do not need to be simulated by an imaginary potential.

To define the fusion component of the potential, we follow the method of Refs. [30, 31], where a short-range absorption potential is included as

$$W_{cc'}(r) = -\frac{W_0}{1+\exp((r-R_0)/a)}\delta_{cc'}. \tag{9}$$

The range R_0 is chosen smaller than the barrier radius, and this potential acts at short distances only. The authors of Refs. [30, 31] have shown that the fusion cross section is virtually insensitive to the choice of the depth W_0 (changing $W_0 = 10$ MeV to $W_0 = 50$ MeV modifies the cross sections by less than 1%). In our multichannel calculation, we take $W_0 = 10$ MeV, $R_0 = 3$ fm, and $a = 0.1$ fm, and we

use the same conditions to investigate the elastic-scattering and fusion processes. We have tested that the cross sections are stable within $1-2\%$ when these parameters are modified. This is illustrated in Fig.2, where we compare the fusion probabilities computed with definitions (8) (dotted lines) and (9) (solid line) at a typical energy $E_{cm} = 4$ MeV. Three values $W_0 = 10, 30, 50$ MeV are considered, and the fusion probabilities are indistinguishable at the scale of the figure. An important consequence is that the model is free of parameters, and that all cross sections are obtained without any adjustment.

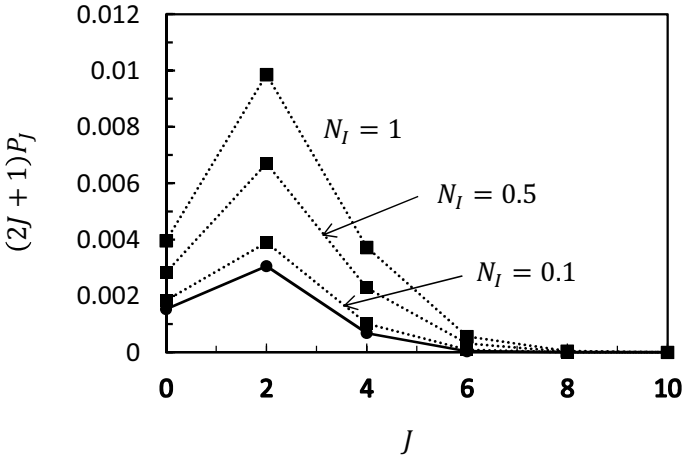

Figure 2. Fusion probabilities computed with definitions (8) (squares, dotted lines) and (9) (circles, solid line) at $E_{cm} = 4$ MeV. Three values $W_0 = 10, 30, 50$ MeV are considered, but the curves are indistinguishable at the scale of the figure.

Our main goal is to investigate the ^{12}C+^{12}C fusion cross section. However, we first assess the accuracy of the model with elastic cross sections, which are well known experimentally at energies close to the Coulomb barrier [23]. The elastic cross sections are computed from the scattering matrices by using standard formulae [16]. The fusion cross section is defined as [32]

$$\sigma_F(E) = \frac{2\pi}{k^2} \sum_{J \text{ even}} (2J+1) P_J(E), \tag{10}$$

where k is the wave number, and where the fusion probability $P_J(E)$ is obtained from

$$P_J(E) = -\frac{2}{\hbar v} \sum_c \int |g_c^{J\pi}(r)|^2 \, W_{cc}(r) \, dr, \tag{11}$$

where v is the relative velocity [16]. At low energies, the fusion and reaction cross sections are identical, and $P_J(E)$ can be expressed as

$$P_J(E) = 1 - |U_{11}^J|^2, \tag{12}$$

where U_{11}^J is the elastic element of the collision matrix, associated with the ^{12}C+^{12}C ground-state channel. These two definitions are strictly identical below the first inelastic channel (open at 4.44 MeV), and this identity provides a strong test of the calculation. At stellar energies (i.e. around 2 MeV or below), $U_{11}^J \approx 1$, and Eq. (12) becomes numerically unstable. Besides its better numerical stability, definition (11) presents another advantage, as the role of the inelastic channels can be evaluated, by computing the individual contributions of each channel c.

3 Elastic scattering and fusion

The present folding model is first applied to ^{12}C+^{12}C elastic scattering at energies around the Coulomb barrier, where experimental data are available [23]. These data can be used to assess the reliability of the model, and hence of the fusion cross sections. Our goal is not to fit the data, and we remind the reader that there is no fitting parameter in the model.

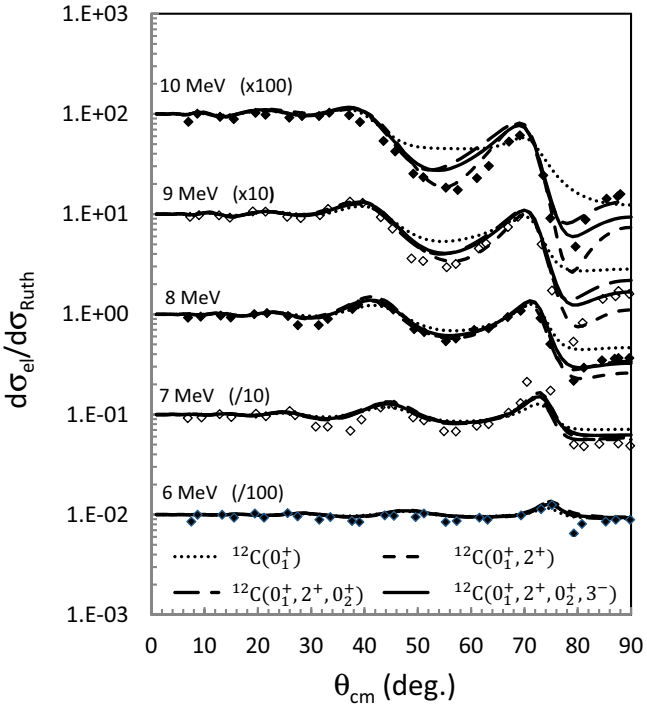

Figure 3. Ratios of the elastic and Rutherford cross sections around the Coulomb barrier, for increasing numbers of ^{12}C+^{12}C inelastic channels. Labels correspond the the c.m. energies. Experimental data are from Ref. [23].

The comparison between theory and experiment is presented in Fig. 3, where we start from a single-channel approximation, and progressively include additional channels. Of course, at 6 MeV, the physics of the problem is essentially determined by the Coulomb interaction and the role of the inelastic channels is hardly visible. When the energy increases, and in particular at $E = 10$ MeV, inelastic channels significantly improve the theoretical cross section. The most sensitive angular range is beyond $\theta = 70°$, where the single-channel approximation provides a poor fit of the data. Including the 2^+ state improves the overall agreement, but adding further the 0_2^+ Hoyle state provides an excellent agreement with the data. Note that good fits can be obtained even in the single-channel approximation [12], but after fitting the imaginary potential to optimize the agreement with experiment.

For the ^{12}C+^{12}C reaction, the fusion cross section is traditionally converted to a modified S factor as

$$\tilde{S}(E) = \sigma_F(E) E \exp(2\pi\eta + 0.46\, E), \tag{13}$$

where η is the Sommerfeld parameter. The linear term in the exponential accounts for an additional energy dependence (E is expressed in MeV). The modified S factor is displayed in Fig. 4, where the

experimental data have been corrected as suggested by Aguilera *et al.* [10]. Above the Coulomb barrier ($\approx$ 6.5 MeV) the data are well reproduced by the calculation, and the role of inelastic channels is minor. When the energy decreases, the sensitivity with respect to the number of excited channels is more and more important, as expected from Ref. [17]. At $E = 1$ MeV, the multichannel calculation provides an enhancement by about a factor of three, in comparison with the single-channel approach. Of course, fluctuations are absent from the present theory. Although molecular resonances are predicted by the calculation with a real potential, they are strongly hindered by the absorption part of the potential.

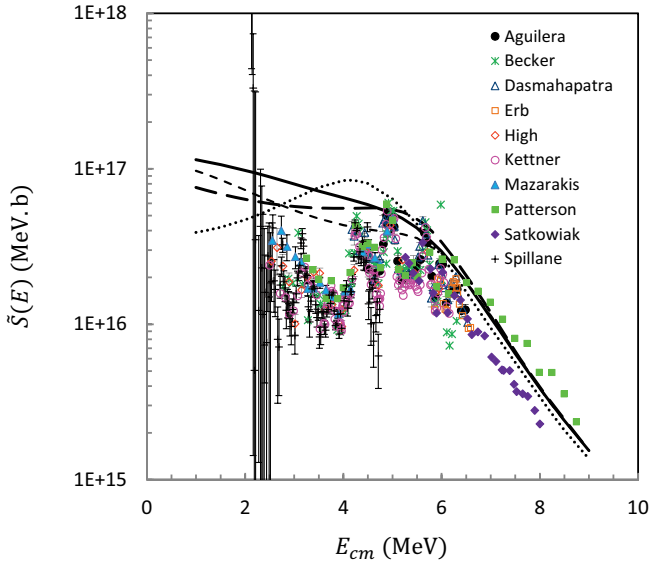

Figure 4. (Color online). Modified S factor (13) for increasing numbers of ^{12}C+^{12}C inelastic channels (the curves are as in Fig. 3). Experimental data are taken from Refs.[10, 33–40].

In order to interpret the theoretical S factor, we present in Fig. 5 a decomposition in angular momenta J (upper panel) and in the various channels (lower panel). The fusion cross section is essentially given by the contributions of $J = 0^+$ and $J = 2^+$; $J = 4^+$ provides less than 10 %, and other partial waves are negligible. The contributions of the different channels confirm that the fusion cross sections are strongly affected by inelastic channels. These channels are closed at low energies, but the corresponding wave functions $g_c^{J\pi}(r)$ have a significant amplitude in the inner region. Even if they tend to zero at large distances, the short-range potential $W(r)$ makes integrals (11) sensitive to the inner part of the wave function only. Consequently the contribution of inelastic channels in the fusion cross section (10) may be important, and even larger than the ground-state contribution. The role of the Hoyle state is supported by the importance of the ^{12}C(0_1^+)+^{12}C(0_2^+) channel, which is even dominant above 3.5 MeV.

4 Conclusion

We have investigated the ^{12}C+^{12}C fusion process in a multichannel model. The coupling potentials are generated from ^{12}C densities obtained in a microscopic cluster model. Our calculation does

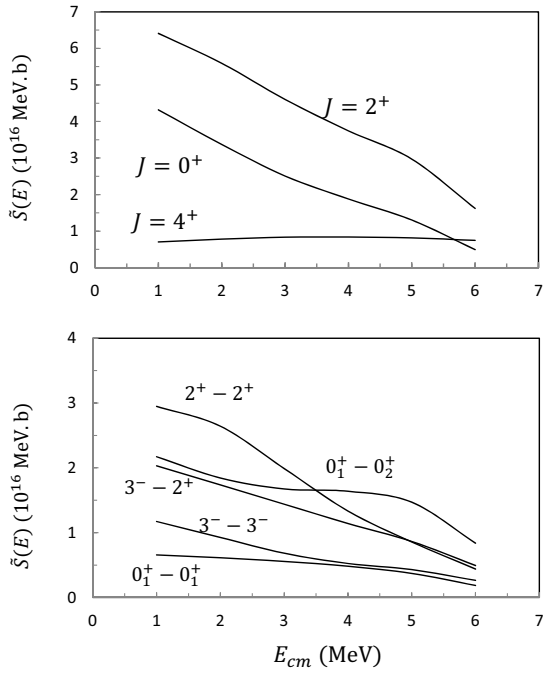

Figure 5. Decompositions of the modified S factor (13) in partial waves (upper panel), and in the main channel contributions (lower panel).

not contain any fitting parameter, and provides simultaneously the fusion and elastic cross sections. Around the Coulomb barrier the elastic data are well reproduced by the model provided that all inelastic channels, and in particular those involving the 0_2^+ state, are included. We confirm the conclusion of Ref. [17], i.e. that inelastic channels play an important role, and must be taken into account for a precise description of the fusion cross section.

A possible improvement would be the introduction of 3α breakup channels. Although the $0_1^+, 2^+, 0_2^+$ and 3^- states, included in the present work, are expected to be the most important excited states, breakup channels may also play a role. Another challenge for future works is to combine this multichannel approach with a consistent description of the broad states observed in the fusion data.

A Appendix

A.1 Densities and form factors

Let us consider a nucleus with wave function Φ^{IK} depending on coordinates $\boldsymbol{r}_i$ (the parity is not written for the sake of simplicity). The density and form factor are defined as

$$\rho_{IK,I'K'}(\boldsymbol{r}) =< \Phi^{IK}| \sum_{i=1}^{A} \delta(\boldsymbol{r} - \boldsymbol{r}_i)|\Phi^{I'K'} >= \frac{1}{(2\pi)^3} \int \exp(-i\boldsymbol{q}\cdot\boldsymbol{r}) F_{IK,I'K'}(\boldsymbol{q}) d\boldsymbol{q}, \tag{A.1}$$

$$F_{IK,I'K'}(\boldsymbol{q}) =< \Phi^{IK}| \sum_{i=1}^{A} \exp(i\boldsymbol{q}\cdot\boldsymbol{r}_i)|\Phi^{I'K'} >= \int \exp(i\boldsymbol{q}\cdot\boldsymbol{r}) \rho_{IK,I'K'}(\boldsymbol{r}) d\boldsymbol{r}. \tag{A.2}$$

These quantities are expanded over multipoles as

$$\rho_{IK,I'K'}(\boldsymbol{r}) = \sum_{\ell} < I'K'\ell m|IK > \rho^{\ell}_{I,I'}(r)\Big(i^{\ell}Y^{m}_{\ell}(\Omega_r)\Big)^{*}, \tag{A.3}$$

$$F_{IK,I'K'}(\boldsymbol{q}) = \sum_{\ell} < I'K'\ell m|IK > F^{\ell}_{I,I'}(q)\Big(i^{\ell}Y^{m}_{\ell}(\Omega_q)\Big)^{*}. \tag{A.4}$$

A simple calculation shows that the multipole components are related by

$$F^{\ell}_{I,I'}(q) = 4\pi \int \rho^{\ell}_{I,I'}(r) j_{\ell}(qr) r^2 dr, \tag{A.5}$$

$$\rho^{\ell}_{I,I'}(r) = \frac{1}{2\pi^2} \int F^{\ell}_{I,I'}(q) j_{\ell}(qr) q^2 dq, \tag{A.6}$$

where $j_\ell(x)$ is a spherical Bessel function.

A.2 General definitions of folding potentials

The Hamiltonian of the system is given by

$$H = T_r + H_0(\boldsymbol{\xi}) + V(\boldsymbol{r},\boldsymbol{\xi}), \tag{A.7}$$

where $\boldsymbol{r}$ is the relative distance between the c.m. of the nuclei, and $\boldsymbol{\xi}$ a set of internal coordinates. In this equation, T_r is the relative kinetic energy, and $H_0(\boldsymbol{\xi})$ is the internal hamiltonian. The interaction term is explicitly given by

$$V(\boldsymbol{r},\boldsymbol{\xi}) = \sum_{i=1}^{A_1} v_{NT}(\boldsymbol{r} - \boldsymbol{r}_i) \text{ for single folding,} \tag{A.8}$$

$$= \sum_{i=1}^{A_1}\sum_{j=1}^{A_2} v_{NN}(\boldsymbol{r} - \boldsymbol{r}_i + \boldsymbol{r}_j) \text{ for double folding,} \tag{A.9}$$

where v_{NT} and v_{NN} are nucleon-target and nucleon-nucleon interactions, respectively.

This potential can be expanded in multipoles as

$$\begin{aligned} V(\boldsymbol{r},\boldsymbol{\xi}) &= \sum_{\lambda\mu} V_{\lambda\mu}(r,\boldsymbol{\xi}) Y^{\mu *}_{\lambda}(\Omega_r) \\ &= \sum_{\lambda} (-1)^{\lambda}\hat{\lambda}\big[V_{\lambda}(r,\boldsymbol{\xi}) \otimes Y_{\lambda}(\Omega_r)\big]^{00}, \end{aligned} \tag{A.10}$$

where we have used the notation $\hat{x} = \sqrt{2x+1}$. A reduced matrix element between channel functions (3) is then given by

$$\begin{aligned} V^{J\pi}_{cc'}(r) =& < \varphi^{J\pi}_{c} \| V(\boldsymbol{r},\boldsymbol{\xi}) \| \varphi^{J\pi}_{c'} > = \sum_{\lambda} (-1)^{\lambda+I'+\ell+J}\hat{\lambda}\hat{I}\hat{\ell} \begin{Bmatrix} I & \ell & J \\ \ell' & I' & \lambda \end{Bmatrix} < Y_{\ell} \| Y_{\lambda} \| Y_{\ell'} > \\ & \times < \big[\Phi^{I_1\pi_1} \otimes \Phi^{I_2\pi_2}\big]^{I} \| V_{\lambda} \| \big[\Phi^{I'_1\pi'_1} \otimes \Phi^{I'_2\pi'_2}\big]^{I'} >, \end{aligned} \tag{A.11}$$

where we have omitted indices α_1 and α_2 for simplicity. The potential matrix element can be evaluated for single and double-folding interactions.

A.3 Single-folding potentials

Let us consider a nucleus with spin I interacting with a structureless target. Then, using (A.10) and the definition of the density, we have

$$< \Phi^{IK}|V_{\lambda\mu}|\Phi^{I'K'} > = \int d\Omega_r Y^{\mu}_{\lambda}(\Omega_r) \int v_{NT}(\boldsymbol{r}-\boldsymbol{s})\,\rho_{IK,I'K'}(\boldsymbol{s})\,d\boldsymbol{s}$$
$$= \frac{1}{(2\pi)^3}\int d\Omega_r Y^{\mu}_{\lambda}(\Omega_r) \int \exp(-i\boldsymbol{q}\cdot\boldsymbol{r})\tilde{v}_{NT}(q)F_{IK,I'K,}(\boldsymbol{q})d\boldsymbol{q}. \quad (A.12)$$

The expansion

$$\exp(-i\boldsymbol{q}\cdot\boldsymbol{r}) = 4\pi\sum_{LM}(-i)^L Y^{M*}_L(\Omega_r)Y^M_L(\Omega_q)j_L(qr) \quad (A.13)$$

provides the reduced matrix element

$$< \Phi^I \|V_\lambda\| \Phi^{I'} >= \frac{(-1)^\lambda}{2\pi^2}\int F^{\lambda}_{I,I'}(q)j_\lambda(qr)\tilde{v}_{NT}(q)q^2dq, \quad (A.14)$$

where $\tilde{v}_{NT}(q)$ is the Fourier transform of the nucleon-target interaction

$$\tilde{v}_{NT}(q) = \int j_0(qr)v_{NT}(r)r^2dr. \quad (A.15)$$

A.4 Double-folding potentials

In this option, both colliding nuclei present a structure defined by their densities. A matrix element of the potential reads

$$< [\Phi^{I_1\pi_1}\otimes\Phi^{I_2\pi_2}]^{IK}|V_{\lambda\mu}|[\Phi^{I'_1\pi'_1}\otimes\Phi^{I'_2\pi'_2}]^{I'K'} >= \sum_{K_1K_2K'_1K'_2} < I_1K_1I_2K_2|IK >< I'_1K'_1I'_2K'_2|I'K' >$$
$$\times\int d\Omega_r Y^{\mu}_{\lambda}(\Omega_r)\int v_{NN}(\boldsymbol{r}-\boldsymbol{s}_1+\boldsymbol{s}_2)\,\rho_{I_1K_1,I'_1K'_1}(\boldsymbol{s}_1)\rho_{I_2K_2,I'_2K'_2}(\boldsymbol{s}_2)\,d\boldsymbol{s}_1\,d\boldsymbol{s}_2. \quad (A.16)$$

This expression provides the reduced matrix element

$$< \left[\Phi^{I_1\pi_1}\otimes\Phi^{I_2\pi_2}\right]^I \|V_\lambda\| \left[\Phi^{I'_1\pi'_1}\otimes\Phi^{I'_2\pi'_2}\right]^{I'} >= \frac{1}{2\pi^2}\sum_{\lambda_1\lambda_2}\hat{I}_1\hat{I}_2\hat{\lambda}_1\hat{\lambda}_2\hat{I}'\frac{1}{\sqrt{4\pi}}(-i)^{\lambda+\lambda_1-\lambda_2}$$
$$\times < \lambda_1 0\lambda_2 0|\lambda 0 > \begin{Bmatrix} I_1 & I_2 & I \\ I'_1 & I'_2 & I' \\ \lambda_1 & \lambda_2 & \lambda \end{Bmatrix}\int F^{\lambda_1}_{I_1,I'_1}(q)F^{\lambda_2}_{I_2,I'_2}(q)j_\lambda(qr)\tilde{v}_{NN}(q)q^2dq. \quad (A.17)$$

Here $\tilde{v}_{NN}(q)$ is the Fourier transform of the nucleon-nucleon interaction. The single-folding definition (A.14) can be easily recovered by neglecting the internal structure of nucleus 2 ($I_2 = I'_2 = 0,\ F^0_{0,0}(q) = \sqrt{4\pi}$).

References

[1] W.D. Arnett, F.K. Thielemann, Astrophys. J. **295**, 589 (1985)

[2] M.E. Bennett, R. Hirschi, M. Pignatari, S. Diehl, C. Fryer, F. Herwig, A. Hungerford, K. Nomoto, G. Rockefeller, F.X. Timmes et al., Mon. Not. R. Astron. Soc **420**, 3047 (2012)
[3] M. Pignatari, R. Hirschi, M. Wiescher, R. Gallino, M. Bennett, M. Beard, C. Fryer, F. Herwig, G. Rockefeller, F.X. Timmes, Astrophys. J. **762**, 31 (2013)
[4] W.A. Fowler, G.R. Caughlan, B.A. Zimmerman, Ann. Rev. Astron. Astrophys. **5**, 525 (1967)
[5] D.D. Clayton, *Principles of stellar evolution and nucleosynthesis* (The University of Chicago Press, 1983)
[6] C. Iliadis, *Nuclear Physics of Stars* (Wiley-VCH Verlag GmbH, 2007)
[7] E. Almqvist, D.A. Bromley, J.A. Kuehner, Phys. Rev. Lett. **4**, 515 (1960)
[8] T. Spillane, F. Raiola, C. Rolfs, D. Schürmann, F. Strieder, S. Zeng, H.W. Becker, C. Bordeanu, L. Gialanella, M. Romano et al., Phys. Rev. Lett. **98**, 122501 (2007)
[9] C.L. Jiang, B.B. Back, H. Esbensen, R.V.F. Janssens, K.E. Rehm, R.J. Charity, Phys. Rev. Lett. **110**, 072701 (2013)
[10] E.F. Aguilera, P. Rosales, E. Martinez-Quiroz, G. Murillo, M. Fernández, H. Berdejo, D. Lizcano, A. Gómez-Camacho, R. Policroniades, A. Varela et al., Phys. Rev. C **73**, 064601 (2006)
[11] A. Diaz-Torres, M. Wiescher, AIP Conf. Proc. **1491**, 273 (2012)
[12] L.R. Gasques, A.V. Afanasjev, E.F. Aguilera, M. Beard, L.C. Chamon, P. Ring, M. Wiescher, D.G. Yakovlev, Phys. Rev. C **72**, 025806 (2005)
[13] R. Perez-Torres, T. Belyaeva, E. Aguilera, Phys. At. Nucl. **69**, 1372 (2006)
[14] P. Christensen, Z. Switkowski, Nucl. Phys. A **280**, 205 (1977)
[15] P. Descouvemont, Nucl. Phys. A **470**, 309 (1987)
[16] L.F. Canto, M.S. Hussein, *Scattering Theory of Molecules, Atoms and Nuclei* (World Scientific Publishing, 2013)
[17] H. Esbensen, X. Tang, C.L. Jiang, Phys. Rev. C **84**, 064613 (2011)
[18] G.R. Satchler, W.G. Love, Phys. Rep. **55C**, 183 (1979)
[19] A. Kobos, B. Brown, P. Hodgson, G. Satchler, A. Budzanowski, Nucl. Phys. A **384**, 65 (1982)
[20] M. Kamimura, Nucl. Phys. A **351**, 456 (1981)
[21] A. Tohsaki, H. Horiuchi, P. Schuck, G. Röpke, Phys. Rev. Lett. **87**, 192501 (2001)
[22] M. Ito, Y. Sakuragi, Y. Hirabayashi, Phys. Rev. C **63**, 064303 (2001)
[23] W. Treu, H. Fröhlich, W. Galster, P. Dück, H. Voit, Phys. Rev. C **22**, 2462 (1980)
[24] M. Assunção, P. Descouvemont, Phys. Lett. B **723**, 355 (2013)
[25] D.T. Khoa, G. Satchler, Nucl. Phys. A **668**, 3 (2000)
[26] P. Descouvemont, D. Baye, Rep. Prog. Phys. **73**, 036301 (2010)
[27] D. Baye, Phys. Stat. Sol. (b) **243**, 1095 (2006)
[28] T. Udagawa, B.T. Kim, T. Tamura, Phys. Rev. C **32**, 124 (1985)
[29] G.R. Satchler, Phys. Rev. C **32**, 2203 (1985)
[30] M. Rhoades-Brown, P. Braun-Munzinger, Phys. Lett. B **136**, 19 (1984)
[31] A. Diaz-Torres, I.J. Thompson, Phys. Rev. C **65**, 024606 (2002)
[32] L.F. Canto, P.R.S. Gomes, R. Donangelo, M.S. Hussein, Phys. Rep. **424**, 1 (2006)
[33] H.W. J. R. Patterson, C.S. Zaidinis, Astrophys. J. **157**, 367 (1969)
[34] M.G. Mazarakis, W.E. Stephens, Phys. Rev. C **7**, 1280 (1973)
[35] M. High, B. Cujec, Nucl. Phys. A **282**, 181 (1977)
[36] K.A. Erb, R.R. Betts, S.K. Korotky, M.M. Hindi, P.P. Tung, M.W. Sachs, S.J. Willett, D.A. Bromley, Phys. Rev. C **22**, 507 (1980)

[37] K. Kettner, H. Lorenz-Wirzba, C. Rolfs, Z. Phys. A **298**, 65 (1980)
[38] H. Becker, K. Kettner, C. Rolfs, H. Trautvetter, Z. Phys. A **303**, 305 (1981)
[39] B. Dasmahapatra, B. Cujec, F. Lahlou, Nucl. Phys. A **384**, 257 (1982)
[40] L.J. Satkowiak, P.A. DeYoung, J.J. Kolata, M.A. Xapsos, Phys. Rev. C **26**, 2027 (1982)